

# Al<sub>2</sub>O<sub>3</sub> Microresonator Based Passive and Active Biosensors

Michiel de Goede<sup>1</sup>, Lantian Chang<sup>1</sup>, Meindert Dijkstra<sup>1</sup>, Raquel Obregón<sup>2</sup>, Javier Ramón-Azcón<sup>2</sup>, Elena Martínez<sup>2</sup>, Laura Padilla<sup>3</sup>, Jaume Adan<sup>3</sup>, Francesc Mitjans<sup>3</sup>, and Sonia M. García-Blanco<sup>1</sup>

<sup>1</sup>Optical Sciences Group, MESA+ Institute for Nanotechnology, University of Twente,  
P.O. Box 217, 7500 AE Enschede, The Netherlands

<sup>2</sup>Institute for Bioengineering of Catalonia, The Barcelona Institute of Science and Technology,  
Baldiri Reixac 10-12, 08028 Barcelona Spain

<sup>3</sup>Health & Biomedicine Unit, LEITAT Technological Center, Baldiri Reixac 15—21, Barcelona 08028, Spain

## ABSTRACT

Al<sub>2</sub>O<sub>3</sub> microresonators were realized for sensing applications of both passive and active devices. Passive microring resonators exhibited quality factors up to  $3.2 \times 10^5$  in air. A bulk refractive index sensitivity of  $\sim 100$  nm/RIU was demonstrated together with a limit of detection of  $\sim 10^{-6}$  RIU. Functionalizing their surface allowed for the label-free detection of the biomarker rhS100A4 from urine with a limit of detection of 3 nM. Furthermore, single-mode Al<sub>2</sub>O<sub>3</sub>:Yb<sup>3+</sup> microdisk lasers were realized that could operate in an aqueous environment. Upon varying the bulk refractive index their lasing wavelength could be tuned with a sensitivity of  $\sim 20$  nm/RIU and a LOD of  $\sim 3 \times 10^{-6}$  RIU.

**Keywords:** aluminium oxide, ytterbium, microresonator, optical sensing.

## 1. INTRODUCTION

Optical microresonators find many applications for on-chip integrated optical biosensors. Their operation is based on monitoring the change of resonance wavelength induced by a dielectric perturbation. Some of the best sensor performances regarding sensitivity, limit of detection and clinically relevant biomarker detection have been demonstrated on SOI [1], Si<sub>3</sub>N<sub>4</sub> [2] and SiON [3] technologies.

As an alternative material technology Al<sub>2</sub>O<sub>3</sub> can be used for such microresonator-based optical sensors. One of the attractive features of Al<sub>2</sub>O<sub>3</sub> is that it can be doped with rare-earth ions to achieve optical gain [4] and lasing [5]. Optical sensing with laser generated light allows for new sensor functionality with simple detection schemes. For instance, a distributed feedback laser was realized that could detect particles through a variation of its beat note [6]. Furthermore, this type of Al<sub>2</sub>O<sub>3</sub> lasers exhibits very high quality factors and narrow laser linewidths [7], allowing for ultra-sensitive operation.

Here, we present an overview of our recent progress on realizing both passive (undoped) and active (doped) optical sensors based on Al<sub>2</sub>O<sub>3</sub> microresonators. A passive sensor based on an Al<sub>2</sub>O<sub>3</sub> microring resonator was shown to be able to detect clinically relevant cancer biomarkers from urine with a limit of detection (LOD) of 3 nM. Furthermore, we present an Al<sub>2</sub>O<sub>3</sub>:Yb<sup>3+</sup> microdisk laser that emits at a single wavelength while operating in an aqueous environment. The device was operated as a sensor by varying the bulk refractive index of deionized water flown over it, inducing a change of the lasing wavelength. Both the passive and active sensor have a bulk refractive index LOD on the order of  $10^{-6}$  RIU. These results indicate the viability of realizing an active sensor platform on the Al<sub>2</sub>O<sub>3</sub> waveguide technology.

## 2. DEVICE FABRICATION

Two sensing devices were designed: an undoped device for operation in the C-band at a wavelength of 1550 nm and one doped with ytterbium for lasing at a wavelength around 1030 nm. For the former a microring resonator was chosen for high sensitivity, for the latter a microdisk resonator for high confinement and low losses to ensure good lasing performance. Both resonators were designed for a radius of 200  $\mu$ m and coupling to a bus waveguide of width 2.2  $\mu$ m. The undoped device has a waveguide thickness of 0.7  $\mu$ m, the doped device is 0.55  $\mu$ m thick.

The fabrication of these devices starts with the deposition of doped and undoped dielectric Al<sub>2</sub>O<sub>3</sub> layers with an AJA ATC reactive sputtering system onto thermally oxidized 100-mm Si wafers. The Yb<sup>3+</sup> dopants are introduced by co-sputtering both from an Al and a Yb target. The waveguides and resonators were then defined with UV lithography and fully etched with an Oxford PlasmaPro 100 Estralas inductively coupled plasma reactive ion etch (Figs. 1a and 1b). A PECVD SiO<sub>2</sub> cladding was then deposited while leaving the resonators open to be addressed in the sensing experiments. After dicing into small chips containing the devices, a PDMS microfluidic device was bonded to them to flow liquids over the sensing chip (Fig. 1c). The final device was connected to a syringe pump, kept at a fixed temperature by a thermostat and butt coupled by two optical fibers (Fig. 1d).

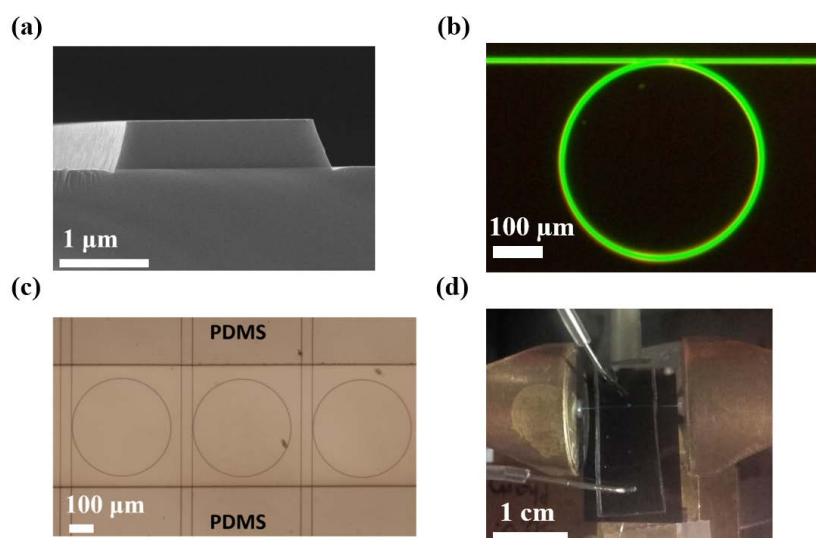


Figure 1: (a)  $\text{Al}_2\text{O}_3$  waveguide cross section; (b) Laser light coupled into microring resonator; (c) Microring resonator inside PDMS microfluidic channel; (d) Optofluidic device containing the sensor chip bonded to PDMS microfluidics.

### 3. PASSIVE MICRORING RESONATOR SENSING

The undoped, passive  $\text{Al}_2\text{O}_3$  microring resonators were characterized with an Agilent 81646 tunable laser around 1550 nm. Their transmission spectrum exhibited resonance dips with quality factors up to  $3.2 \times 10^5$  for TE polarization in air, corresponding with propagation losses of  $0.6 \pm 0.04$  dB/cm. Flowing deionized water over the device lowered their quality factors to  $\sim 5 \times 10^4$  with propagation losses of  $\sim 5$  dB/cm due to water absorption loss.

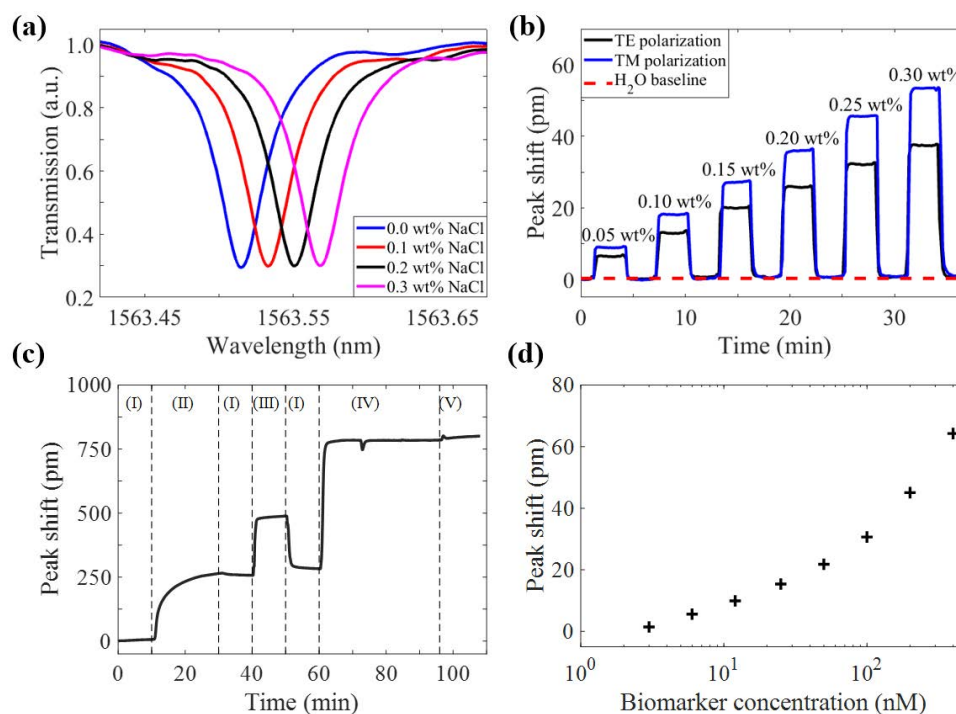


Figure 2: (a) Resonance wavelength shift induced by change of bulk refractive index sensing; (b) Real-time bulk refractive index sensing; (c) Biosensing sensorgram of various liquids flown over the device: (I) PBS, (II) PBS containing monoclonal antibodies, (III) PBS containing BSA, (IV) urine, (V) urine containing the biomarker; (d) Total shift as function of biomarker concentration.

A microring resonator was used as a bulk refractive index sensor by monitoring the shift of the resonance wavelength while flowing deionized water containing varying concentrations of NaCl over it (Fig. 2a). Repeatedly recording a transmission spectrum and following the location of the resonance peaks on it allowed for real-time monitoring the sensor output (Fig. 2b). A bulk refractive index sensitivity of  $102.3 \pm 0.5$  nm/RIU

was measured for TM polarization. Combined with the uncertainty of the sensor's output and noise, a LOD of  $1.1 \times 10^{-6}$  RIU was achieved.

The device was used as a biosensor by applying a surface functionalization to its surface to immobilize anti-S100A4 monoclonal antibodies onto it (Fig. 2c). Urine containing the label-free biomarker rhS100A4 was flown over the microring resonator to demonstrate binding thereof to the antibodies (Fig. 2d). A lowest concentration of 3 nM was detected, which is within the clinically relevant range [8].

#### 4. ACTIVE MICRODISK RESONATOR SENSING

The  $\text{Al}_2\text{O}_3:\text{Yb}^{3+}$  microdisk resonator was designed for operation around at a wavelength of 1000 nm, since  $\text{Yb}^{3+}$  has an absorption peak around 976 nm and an emission peak around 1020 – 1060 nm. The microdisk resonator was optically pumped with a diode at 976 nm while deionized water was flown over it. The device exhibited lasing at a single wavelength with a side-mode suppression ratio of almost 30 dBm (Fig. 3a).

Figure 3b shows the power characteristics of the laser. The device has a threshold of around 7 mW. Since there are coupling losses for the fiber-to-chip coupling, the threshold for power injected into the chip is approximately 2 mW. Likewise, the uncorrected slope efficiency is around 0.1%, whereas compensating for the coupling loss gives a slope efficiency of  $\sim 2\%$  for lasing power generated on the chip over pump power injected into the chip.

To demonstrate how the microdisk resonator could be used as a sensor, methanol, ethanol and deionized water were flown over the device while monitoring the lasing wavelength (Fig. 3c). This shifted to higher values for a higher refractive index of the fluid and allowed for a tuning range of  $\sim 5$  nm. To inspect more closely the bulk refractive index sensitivity, the emitted light was mixed with that of an external Toptica CTL 1050 laser closely tuned to the microdisk's emission wavelength and guided to a RF analyzer. By mixing the two signals a low-frequency beat note is formed that can be recorded with the RF analyzer. Flowing deionized water containing salt over the microdisk resonator changes its lasing wavelength, resulting in a variation of beat note (Fig. 3d). For this device a bulk refractive index sensitivity of  $21.3 \pm 0.8$  nm/RIU was determined together with a LOD of  $3.4 \times 10^{-6}$  RIU. The microdisk resonator's sensitivity is lower than that of the microring resonator due to a stronger modal confinement. Currently this experimental procedure is applied to test the microdisk as a biosensor for biomarker detection.

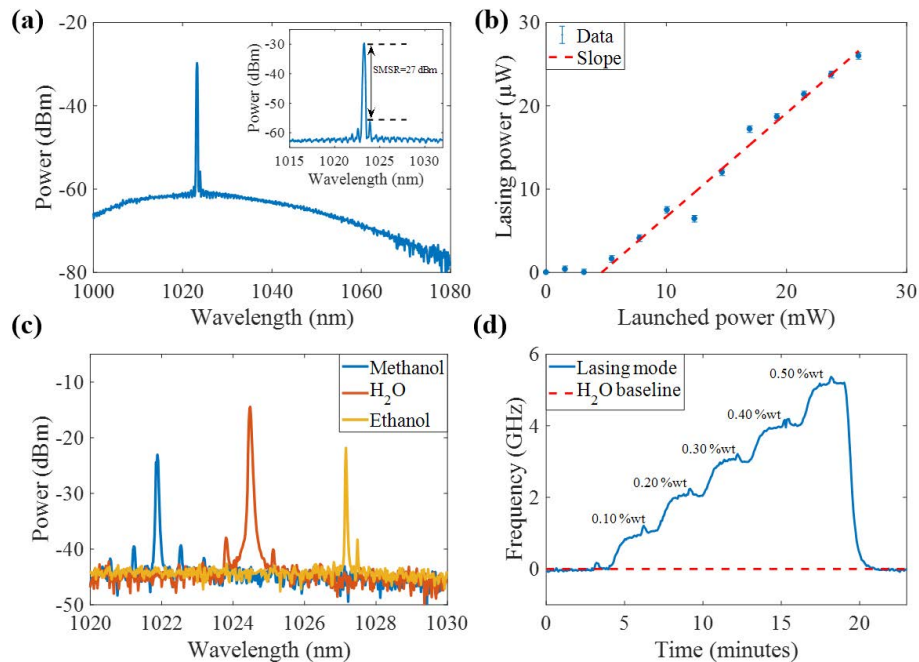


Figure 3: (a)  $\text{Al}_2\text{O}_3:\text{Yb}^{3+}$  microdisk lasing spectrum. Inset shows zoom of the lasing peak; (b) Light-light curve of the laser; (c) Tuning of the lasing wavelength by varying the bulk refractive index; (d) Real-time active sensing of bulk refractive index variation.

#### 5. CONCLUSION

Doped and undoped  $\text{Al}_2\text{O}_3$  resonators were fabricated to be used for respectively active and passive sensing experiments. High quality factor passive microring resonators were realized for label-free cancer biomarker detection from urine down to concentrations of 3 nM. An active microdisk lasers was shown that operates at a single mode lasing wavelength, which could be used as a sensor by tuning the refractive index of the top cladding while monitoring the change of emission wavelength. Both results indicate the viability of using the

Al<sub>2</sub>O<sub>3</sub> waveguide technology for optical sensing on passive and active platforms. The latter has the prospect of ultra-sensitive, simple detection schemes biosensor operation.

#### ACKNOWLEDGEMENTS

This project has received funding from the European Union's Horizon 2020 research and innovation programme under grant agreement No 634928.

#### REFERENCES

- [1] W. Bogaerts *et al.*, "Silicon microring resonators," *Laser Photon. Rev.* **6**, 47-73 (2011).
- [2] K. Wörhoff *et al.*, "TriPleX: A versatile dielectric photonic platform," *Adv. Opt. Technol.* **4**, 189-207 (2015).
- [3] A. Samusenko *et al.*, "A SiON microring resonator-based platform for biosensing at 850 nm," *J. Light. Technol.* **34**, 969-977 (2016).
- [4] K. Wörhoff *et al.*, "Reliable low-cost fabrication of low-loss Al<sub>2</sub>O<sub>3</sub>:Er<sup>3+</sup> waveguides with 5.4-dB optical gain," *IEEE J. Quantum Electron.* **45**, 454-461 (2009).
- [5] J. Bradley *et al.*, "Integrated Al<sub>2</sub>O<sub>3</sub>:Er<sup>3+</sup> ring lasers on silicon with wide wavelength selectivity," *Opt. Lett.* **35**, 73-75 (2010).
- [6] E. Bernhardt *et al.*, "Intra-laser-cavity microparticle sensing with a dual-wavelength distributed-feedback laser," *Laser Photonics Rev.* **7**, 589-598 (2013).
- [7] E. Bernhardt *et al.*, "Photonic generation of stable microwave signals from a dual-wavelength Al<sub>2</sub>O<sub>3</sub>:Yb<sup>3+</sup> distributed-feedback waveguide laser," *Opt. Lett.* **37**, 181-183 (2012).
- [8] J.L. Turnier *et al.*, "Urine S100 proteins as potential biomarkers of lupus nephritis activity," *Arthritis Res. Ther.* **19**, 242-253 (2017).